JACS
JOURNAL OF THE AMERICAN CHEMICAL SOCIETY

Communication

pubs.acs.org/JACS

Surfactant-Directed Synthesis of Mesoporous Pd Films with Perpendicular Mesochannels as Efficient Electrocatalysts

Cuiling Li,[†] Bo Jiang,[†,‡] Nobuyoshi Miyamoto,[§] Jung Ho Kim,[∥] Victor Malgras,[†] and Yusuke Yamauchi*[,†,‡]

[†]World Premier International (WPI) Research Center for Materials Nanoarchitectonics (MANA), National Institute for Materials Science (NIMS), 1-1 Namiki, Tsukuba, Ibaraki 305-0044, Japan

[‡]Faculty of Science and Engineering, Waseda University, 3-4-1 Okubo, Shinjuku, Tokyo 169-8555, Japan

[§]Department of Life, Environment and Materials Science, Fukuoka Institute of Technology (FIT), 3-30-1 Wajiro-Higashi, Higashi, Fukuoka 811-0295, Japan

[∥]Institute for Superconducting and Electronic Materials, Australian Institute for Innovative Materials, University of Wollongong, Squires Way, North Wollongong, New South Wales 2500, Australia

Supporting Information

ABSTRACT: Palladium (Pd) films with perpendicularly aligned mesochannels are expected to provide fascinating electrocatalytic properties due to their low diffusion resistance and the full utilization of their large surface area. There have been no studies on such mesoporous metal films, because of the difficulties in controlling both the vertical alignment of the molecular template and the crystal growth in the metallic pore walls. Here we report an effective approach for the synthesis of mesoporous Pd films with mesochannels perpendicularly aligned to the substrate by an elaborated electrochemical deposition. The films show a superior electrocatalytic activity by taking full advantage of the perpendicularly aligned mesochannels.

Surfactant assembly provides a general way for preparing ordered mesoporous materials.[1] Many mesoporous materials with different mesostructures and morphologies have been obtained by optimizing the synthetic conditions. Even a same surfactant can result in different mesopore arrangements by changing the concentration. Among various morphologies, mesoporous films have sparked many keen interests in a wide range of potential applications (e.g., catalysis, energy storage, photonic therapy) due to their high accessible active surface, superior structural stability, and unique functions.[2] In general, the surfactant micelles tend to orient parallel to the substrate in order to reduce the surface energy at the interface, resulting in mesochannels inevitably oriented parallel to the substrate and making the internal mesopores inaccessible. Considering practical applications, a precise control over the mesopore orientation is a critical issue to overcome in order to fully exploit the internal pores. Perpendicularly oriented mesochannels in films are an ideal structure which allows the diffusion of reagents from the exterior region to the inner parts, thus favoring the high utilization efficiency brought by the mesopores.[3] Although several strategies employing high magnetic field,[4] electro-assisted self-assembly,[5] air flow,[6] confined effect,[7] and optimal evaporation-induced self-assembly (EISA)[8] have been previously employed for achieving vertically oriented mesochannels, the compositions of the pore walls have been mostly limited to silica, carbons, organosilica, titania, and alumina. To the best of our knowledge, there have been no reports on metal films with perpendicular mesochannels.

Mesoporous metal films possess a high surface area and their fairly stable metallic frameworks provide a large number of catalytically active sites, thereby exhibiting fascinating catalytic properties.[9] Palladium (Pd) has been well-known as an exceptional catalyst for a rich variety of applications, including oxidation of fuels, carbon−carbon coupling reactions, and hydrogen storage/detections.[10] Therefore, mesoporous Pd films with perpendicular mesochannels can bring out many superior electrochemical applications which cannot be achieved by other previously reported mesoporous films.[4−8] Although several approaches using lyotropic liquid crystals, surfactant micelles, or hard-templates have been utilized for the preparation of mesoporous metals,[11] mesoporous metal films with perpendicular mesochannels have never been achieved.

Herein, we report a sophisticated amperometric approach which reduces the Pd species decorated on the surface of the micelles, leading to the formation of continuous Pd films with vertically aligned mesochannels. The resulting mesoporous Pd films distinctly exploit the ultrahigh surface area ensued from the mesoporous architecture and clearly exhibit linearly increasing electrocatalytic activities with increasing the film thickness. In this work, a solution containing cationic surfactant, cetylmethylammonium chloride (C_{16}TAC), and Na_2PdCl_4 was first prepared and used as electrolyte. Then, a conductive Au substrate was employed as a working electrode for the electrodeposition of Pd film at a constant potential under optimized conditions [see Supporting Information (SI) for details]. After completely removing the surfactants, Pd films with perpendicular mesochannels were obtained.

The top surface and cross-section of the obtained films were studied by scanning electron microscope (SEM) and transmission electron microscopy (TEM). From the top-view, uniformly sized mesopores are distinctly distributed over the

Received: June 17, 2015
Published: August 25, 2015

DOI: 10.1021/jacs.5b06278
J. Am. Chem. Soc. 2015, 137, 11558−11561

entire area of the film without any defects, cracks, or bumps (Figures 1a,b and S1). The size of the mesopores is

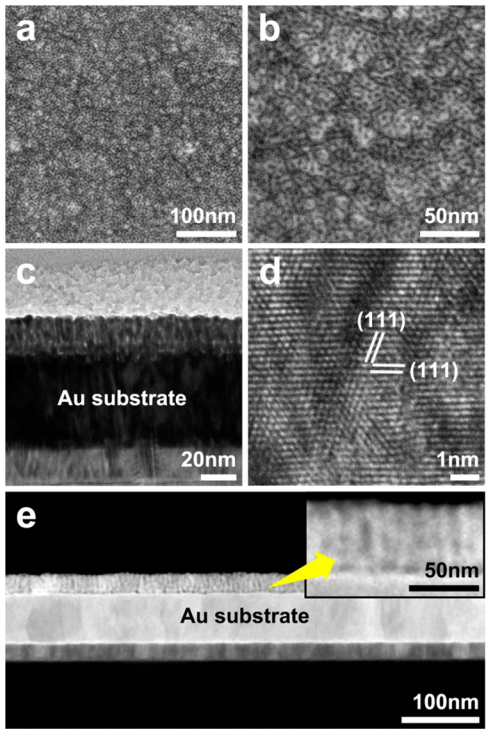

Figure 1. (a, b) SEM images of the top-surface of the obtained Pd films. (c–e) Cross-sectional TEM images of the obtained Pd films [(c) bright-field TEM, (d) high-resolution TEM, and (e) HAADF-STEM images].

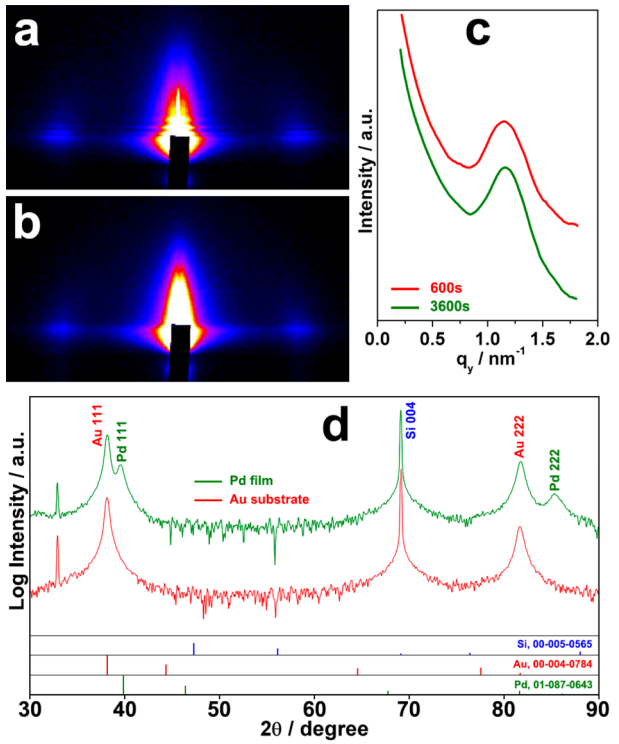

Figure 2. (a, b) 2D GI-SAXS patterns of the obtained Pd films with perpendicular mesochannels after different deposition times of (a) 600 and (b) 3600 s. (c) Intensity profile collected in the in-plane direction against q value. (d) Wide-angle XRD patterns of bare Au substrate and the obtained Pd film with perpendicular mesochannels prepared for a deposition time of 600 s.

homogeneously distributed with a predominant pore size of 2.1 ± 0.2 nm separated by pore walls of 3.3 ± 0.2 nm. Various mesoporous materials have been synthesized using cetylmethylammonium chloride/bromide (C_{16}TAC/C_{16}TAB) with the same hydrocarbon chain length as the pore directing agents. The pore size obtained in this study is well consistent with the ones reported previously (Table S1). The cross-sectional TEM image and the high-angle annular dark-field scanning TEM (HAADF-STEM) image show that cylindrical channels are distributed perpendicularly to the substrate (Figure 1c–e, and S2). In the high-resolution TEM image, it can be observed that the framework is highly crystallized without any amorphous domains, although the lattice fringes can be slightly distorted at certain locations (Figures 1d and S3). The clear lattice fringes with a constant d spacing of 0.225 nm can be ascribed to the (111) lattice planes of face-centered cubic (fcc) Pd crystals. A uniform thickness of 24 nm was distinctly grown on the Au surface (Figures 1c and S4). Although the long-range in-plane ordering of the mesochannels seems limited (Figure S5), the mesochannels are all perpendicularly aligned to the substrate.

Two-dimensional (2D) grazing-incidence small-angle X-ray scattering (GI-SAXS) was employed to further confirm the orientation of mesochannels (Figure 2a–c). The two intense spots correspond to the in-plane periodicity of the obtained films (Figure 2a). The absence of out-of-plane periodicity can rule out any possibility of other three-dimensional mesostructures.[12] The intensity profile collected in the in-plane direction plotted against q value (Figure 2c) reveals a peak centered at q = 1.17 nm^{-1} corresponding to a pore-to-pore d-spacing of 5.4 nm. Considering the wall thickness (~3.3 nm) and the pore size (~2.1 nm), the GI-SAXS data are in good agreement with the SEM results (Figures S1 and S5).

Conceptually different from the EISA method which is generally utilized for preparing mesoporous films,[13] the electrodeposition approach used in this work allows an easy control over the film thickness by changing the deposition time. From the cross-sectional images study, the film thickness was determined to increase linearly with the deposition time, with an average growth rate of 0.076 nm s^{-1} (Figure S6). The 2D GI-SAXS spots are unaffected by increasing the deposition time (Figure 2b,c), suggesting that any film thicknesses can be obtained by choosing a suitable deposition time without interfering with the perpendicularly aligned mesoporous structures. No changes in the vertically aligned mesochannels can be observed even after increasing the deposition time up to 7200 s (leading to a film thickness of 540 nm) (Figure S7).

From the energy dispersive X-ray spectroscopy analysis, it can be observed that the obtained mesoporous films consist of only Pd (not shown). Detailed investigation of the crystalline structure and the preferred orientation inside the Pd films was obtained by wide-angle X-ray diffraction (XRD) carried out in out-of-plane mode, which is sensitive to the lattice parameter in the growth direction. The XRD patterns obtained from the electrodeposited films only gave two diffraction peaks assigned to the (111) and (222) diffraction planes of fcc Pd (JCPDS no. 87-643) (Figure 2d), indicating that the Pd crystals have a preferential orientation according to the (111) plane parallel to the substrate on the seed layer (Au). The Pd crystal growth along the [111] direction is consistent with TEM result (Figure 1d).

DOI: 10.1021/jacs.5b06278
J. Am. Chem. Soc. 2015, 137, 11558–11561

The surfactant assembly, which is usually concentration dependent, is critical to determine the final mesoporous structure. As the surfactant concentration increases, the surfactant assembly changes from free surfactants to spherical and cylindrical micelles.[14] In our system, the concentration of C_{16}TAC is 43 mM, which is higher than its critical micelle concentration (CMC, 16 mM), suggesting the formation of spherical micelles in the electrolyte (Figure S8). It has been known that the strongly charged anionic inorganic species interact with the cationic surfactants.[15] The interactions between the C_{16}TAC micelles and the Pd precursors in the electrolyte were studied by ultraviolet-visible spectroscopy (UV−Vis) absorption (Figure S9). The $[PdCl_4]^{2-}$ species exhibit two absorption maxima at 210 and 235 nm.[16] After being mixed with C_{16}TAC micelle solution, a significant change is observed with the newly formed absorption bands at 226 and 285 nm, which are attributed to the interactions between the anionic $[PdCl_4]^{2-}$ species and the cationic $[C_{16}TA]^{+}$ surfactants.[16] From the SAXS measurement of the electrolyte after the addition of $[PdCl_4]^{2-}$ species, it is found that the spherical micelles are well retained (Figure S8). It is probable that the spherical micelles decorated with $[PdCl_4]^{2-}$ species approach the working electrode when an exterior potential is applied. The Pd species are initially reduced on the surface of the working electrode. Due to its reduction, each $[PdCl_4]^{2-}$ releases four chloride ions, which then probably bind to the surfactants more strongly and induce the sphere-to-rod transition. The formed rod-like micelles can be well oriented perpendicularly on its surface due to the stronger affinity with the hydrophobic core than the hydrophilic shell of the micelles, although cylinder micelles and lamellar phases generally have a strong tendency to align parallel to the substrate surface due to their lower energy.[17] The subsequent Pd deposition and reassembly of surfactant molecules lead to a continuous growth along the longitudinal direction of the cylindrical micelles perpendicularly orientated on the substrate (Figure S10).

The retention of the ordered architecture formed by the surfactant assembly is critical for designing the pore walls. In the case of metals, their crystallized walls are formed simultaneously with the reduction of metal species, unlike post-treated crystallized/graphitized pore walls. In the present system, the crystal growth can be controlled by tuning the reduction conditions. Especially, electrochemical reduction is useful for strict control of the growth speed and the crystallinity of the deposited metals. Various constant potentials in the range of −0.5 and 0.3 V (vs Ag/AgCl) were employed for the electrodeposition of Pd films. The mesoporous structures in the obtained films were studied by SEM and 2D GI-SAXS (Figure S11). During the formation of mesoporous metals, the reduced metal atoms are primarily formed at the hydrophilic region of the micelles where they agglomerate and coalesce until a thick wall is obtained, giving the structure enough mechanical stability. A slow reduction reaction generally allows the surfactant templates to be distorted so large crystals can grow.[18] When a high potential is applied (e.g., 0.2 V, and 0.3 V (vs Ag/AgCl) in the present work), the reduction of the Pd precursors becomes slower, and the mesoporous structures cannot be achieved (Figure S11a,b). Therefore, an appropriate reduction rate is necessary for the preparation of mesoporous metals. Well-ordered mesoporous structures can be obtained when a potential in the range of 0.1 V and −0.1 V (vs Ag/AgCl) is applied, as evidenced by the top-surface SEM images and the 2D GI-SAXS profiles (Figure S11c−e). When the reduction rate is further increased, the initially formed Pd crystals are larger and end up exceeding the size of the hydrophilic volume of the micelles, destroying the ordering of the micelle assembly (Figure S11f−h).[19] From the above results, a moderate potential [i.e., −0.1, 0, and 0.1 V (vs Ag/AgCl)] is essential to control the Pd reduction rate without interfering with the micelle assembly. The surfactant concentration is also critical (Figure S12). When it is lower than the CMC, no porous constructions can be observed, while highly increased concentration (five or ten times higher than the optimal concentration) leads to the formation of perpendicular mesochannels, but with a slightly reduced periodicity.

Motivated by the fact that the perpendicularly aligned mesochannels have naturally a superior mass transport than other architectures, electrochemical measurements were carried out. Here, cyclic voltammograms (CVs) in a 0.5 M H_2SO_4 solution were first performed on the obtained Pd films with various thicknesses. A noticeable current increase in the hydrogen and oxygen adsorption/desorption regions was observed (Figure 3a). The electrochemical surface area

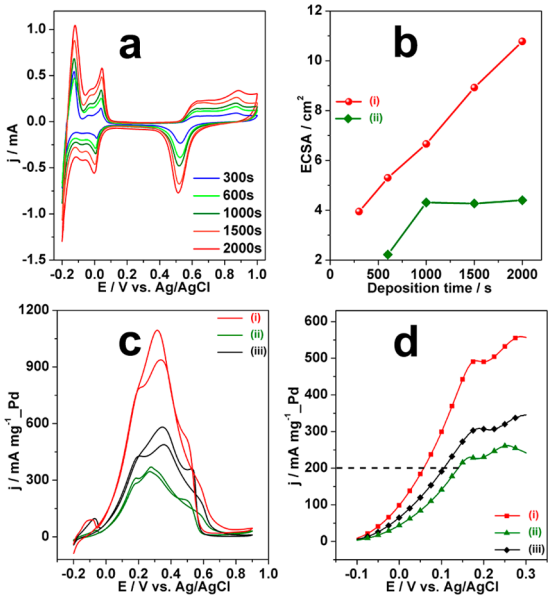

Figure 3. (a) CVs in 0.5 M H_2SO_4 of the obtained Pd films with perpendicular mesochannels with various film thicknesses (the deposition times are 300, 600, 1000, 1500, 2000, respectively). (b) Relationship between the ECSAs and the deposition times. The mesoporous Pd film (i) is compared to a nonporous Pd film (ii). (c) CV curves and (d) potential dependent steady-state current density for formic acid oxidation catalyzed by a Pd film with perpendicular mesochannels (i), a nonporous Pd film (ii), and a commercially available PdB catalyst (iii). The formic acid oxidation reaction is performed in 0.5 M H_2SO_4 containing 0.5 M HCOOH.

(ECSA) was calculated by using the method proposed by Woods (see SI for details). The ECSA was determined to increase linearly with the film thickness (i.e., deposition time), unlike the nonporous Pd films prepared without surfactants (Figures 3b and S13). The volume-normalized ECSA of the Pd film with perpendicular mesochannels is calculated to be 737 $m^2 \cdot cm^{-3}$, which is much higher than that of the mesoporous Pt films prepared from lyotropic liquid crystals (at most 460 $m^2 \cdot cm^{-3}$).[20] Thus, it is found that perpendicularly oriented mesochannels are able to make the whole inner porous structure accessible.

To gain deeper insights regarding the electrocatalytic properties of the Pd films with perpendicular mesochannels, formic acid (HCOOH) oxidation reaction was selected as a

DOI: 10.1021/jacs.5b06278
J. Am. Chem. Soc. 2015, 137, 11558−11561

model reaction. The mesoporous Pd film was evaluated and compared to a nonporous Pd film and a commercially available Pd black (PdB) catalyst. The typical CV curves for HCOOH oxidation catalyzed by different catalysts are shown in Figure 3c. It can be clearly observed that the Pd film with perpendicular mesochannels shows a higher current density of 934.6 mA mg^{-1}_Pd, which is around 2.7 and 1.9 times higher than those of the nonporous Pd film (343.0 mA mg^{-1}_Pd) and the PdB (485.8 mA mg^{-1}_Pd), respectively. In addition, the steady-state current densities obtained on the three different catalysts are also compared (Figure 3d). At a given oxidation current density, as indicated by the dashed line in Figure 3d, the corresponding potential on the mesoporous Pd film is much lower than that on the nonporous Pd film and the PdB. The potential on the mesoporous Pd film is negatively shifted by ∼80 and ∼50 mV, compared with the nonporous Pd film and PdB catalyst, respectively. Thus, the mesoporous Pd film with perpendicular mesochannels exhibits a strongly enhanced catalytic activity (i.e., enhanced Pd utilization efficiency). This is probably attributed to a higher active surface caused by the accessible mesochannels perpendicularly aligned to the substrate.

In this work, we demonstrated a novel approach for the successful preparation of Pd films with perpendicular mesochannels. The pore size is uniform, and straight mesochannels are evenly distributed in the entire area of the obtained films regardless the substrate sizes. A highly enhanced electrocatalytic performance toward formic acid oxidation was observed. The present approach is not only highly reliable and effective for creating vertically aligned mesoporous Pd electrocatalysts but also paves the way for other metals and alloys toward achieving a superior catalytic activity.

■ ASSOCIATED CONTENT

Supporting Information

The Supporting Information is available free of charge on the ACS Publications website at DOI: 10.1021/jacs.5b06278.

Experimental details and additional data (PDF)

■ AUTHOR INFORMATION

Corresponding Author

*Yamauchi.Yusuke@nims.go.jp

Notes

The authors declare no competing financial interest.

■ ACKNOWLEDGMENTS

This research is partially supported by the Grants-in-Aid for Young Scientists A (Research Project Number: 26708028) for the Promotion of Science (JSPS), Japanese-Taiwanese Cooperative Program of the Japan Science and Technology Agency (JST), and The Canon Foundation.

■ REFERENCES

(1) (a) Sakamoto, Y.; Kaneda, M.; Terasaki, O.; Zhao, D.; Kim, J. M.; Stucky, G.; Shin, H. J.; Ryoo, R. *Nature* **2000**, *408*, 449. (b) Suteewong, T.; Sai, H.; Cohen, R.; Wang, S.; Bradbury, M.; Baird, B.; Gruner, S. M.; Wiesner, U. *J. Am. Chem. Soc.* **2011**, *133*, 172. (c) Crepaldi, E. L.; Soler-Illia, G. J. A. A.; Grosso, D.; Cagnol, F.; Ribot, F.; Sanchez, C. *J. Am. Chem. Soc.* **2003**, *125*, 9770. (d) Zhao, D.; Feng, J.; Huo, Q.; Melosh, N.; Fredrickson, G. H.; Chmelka, B. F.; Stucky, G. D. *Science* **1998**, *279*, 548. (e) Han, L.; Miyasaka, K.; Terasaki, O.; Che, S. *J. Am. Chem. Soc.* **2011**, *133*, 11524.

(2) Wu, K. C. W.; Jiang, X.; Yamauchi, Y. *J. Mater. Chem.* **2011**, *21*, 8934.

(3) (a) Feng, X.; Liu, Z.; Hsieh, M.; Chen, M.; Liu, P.; Chen, C.; Zheng, N. *ACS Nano* **2012**, *6*, 4434. (b) Lin, M.; Huang, C.; Lo, M.; Mou, C. *J. Phys. Chem. C* **2008**, *112*, 867. (c) Teng, Z.; Zheng, G.; Dou, Y.; Li, W.; Mou, C.; Zhang, X.; Asiri, A. M.; Zhao, D. *Angew. Chem., Int. Ed.* **2012**, *51*, 2173. (d) Chen, B. C.; Lin, H. P.; Chao, M. C.; Mou, C. Y.; Tang, C. Y. *Adv. Mater.* **2004**, *16*, 1657.

(4) (a) Tolbert, S. H.; Firouzi, A.; Stucky, G. D.; Chmelka, B. F. *Science* **1997**, *278*, 264. (b) Yamauchi, Y.; Sawada, M.; Komatsu, M.; Sugiyama, A.; Osaka, T.; Hirota, N.; Sakka, Y.; Kuroda, K. *Chem. - Asian J.* **2007**, *2*, 1505. (c) Yamauchi, Y.; Sawada, M.; Noma, T.; Ito, H.; Furumi, S.; Sakka, Y.; Kuroda, K. *J. Mater. Chem.* **2005**, *15*, 1137.

(5) (a) Walcarius, A.; Sibottier, E.; Etienne, M.; Ghanbaja, J. *Nat. Mater.* **2007**, *6*, 602. (b) Guillemin, Y.; Etienne, M.; Aubert, E.; Walcarius, A. *J. Mater. Chem.* **2010**, *20*, 6799. (c) Cheng, J.; Rathi, S. J.; Stradins, P.; Frey, G. L.; Collins, R. T.; Williams, S. K. R. *RSC Adv.* **2014**, *4*, 7627.

(6) Shan, F.; Lu, X.; Zhang, Q.; Wu, J.; Wang, Y.; Bian, F.; Lu, Q.; Fei, Z.; Dyson, P. J. *J. Am. Chem. Soc.* **2012**, *134*, 20238.

(7) (a) Lu, Q.; Gao, F.; Komarneni, S.; Mallouk, T. E. *J. Am. Chem. Soc.* **2004**, *126*, 8650. (b) Yamauchi, Y.; Nagaura, T.; Inoue, S. *Chem. - Asian J.* **2009**, *4*, 1059.

(8) Ma, C.; Han, L.; Jiang, Z.; Huang, Z.; Feng, J.; Yao, Y.; Che, S. *Chem. Mater.* **2011**, *23*, 3583.

(9) (a) Fujita, T.; Guan, P.; McKenna, K.; Lang, X.; Hirata, A.; Zhang, L.; Tokunaga, T.; Arai, S.; Yamamoto, Y.; Tanaka, N.; Ishikawa, Y.; Asao, N.; Yamamoto, Y.; Erlebacher, J.; Chen, M. *Nat. Mater.* **2012**, *11*, 775. (b) Warren, S. C.; Messina, L. C.; Slaughter, L. S.; Kamperman, M.; Zhou, Q.; Gruner, S. M.; DiSalvo, F. J.; Wiesner, U. *Science* **2008**, *320*, 1748. (c) Choi, K. S.; McFarland, E. W.; Stucky, G. D. *Adv. Mater.* **2003**, *15*, 2018.

(10) (a) Zhang, H.; Jin, M.; Xiong, Y.; Lim, B.; Xia, Y. *Acc. Chem. Res.* **2013**, *46*, 1783. (b) Lee, H.; Habas, S. E.; Somorjai, G. A.; Yang, P. *J. Am. Chem. Soc.* **2008**, *130*, 5406. (c) Yin, L. X.; Liebscher, J. *Chem. Rev.* **2007**, *107*, 133. (d) Li, G.; Kobayashi, H.; Dekura, S.; Ikeda, R.; Kubota, Y.; Kato, K.; Takata, M.; Yamamoto, T.; Matsumura, S.; Kitagawa, H. *J. Am. Chem. Soc.* **2014**, *136*, 10222.

(11) (a) Attard, G. S.; Bartlett, P. N.; Coleman, N. R. B.; Elliott, J. M.; Owen, J. R.; Wang, J. H. *Science* **1997**, *278*, 838. (b) Wang, H.; Jeong, H. Y.; Imura, M.; Wang, L.; Radhakrishnan, L.; Fujita, N.; Castle, T.; Terasaki, O.; Yamauchi, Y. *J. Am. Chem. Soc.* **2011**, *133*, 14526.

(12) Miyata, H.; Suzuki, T.; Fukuoka, A.; Sawada, T.; Watanabe, M.; Noma, T.; Takada, K.; Mukaide, T.; Kuroda, K. *Nat. Mater.* **2004**, *3*, 651.

(13) (a) Soler-Illia, G. J. A. A.; Angelomé, P. C.; Fuertes, M. C.; Grosso, D.; Boissiere, C. *Nanoscale* **2012**, *4*, 2549. (b) Brezesinski, T.; Wang, J.; Polleux, J.; Dunn, B.; Tolbert, S. H. *J. Am. Chem. Soc.* **2009**, *131*, 1802.

(14) Stein, A.; Rudisill, S. G.; Petkovich, N. D. *Chem. Mater.* **2014**, *26*, 259.

(15) (a) Huo, Q.; Margolese, D. I.; Ciesla, U.; Demuth, D. G.; Feng, P.; Gier, T. E.; Sieger, P.; Firouzi, A.; Chamelka, B. F.; Schüth, F.; Stucky, G. D. *Chem. Mater.* **1994**, *6*, 1176. (b) Monnier, A.; Schüth, F.; Huo, Q.; Kumar, D.; Margolese, D.; Maxwell, R. S.; Stucky, G. D.; Krishnamurty, M.; Petroff, P.; Firouzi, A.; Janicke, M.; Chmelka, B. F. *Science* **1993**, *261*, 1299.

(16) Berhault, G.; Bausach, M.; Bisson, L.; Becerra, L.; Thomazeau, C.; Uzio, D. *J. Phys. Chem. C* **2007**, *111*, 5915.

(17) Kao, K. C.; Lin, C. H.; Chen, T. Y.; Liu, Y. H.; Mou, C. Y. *J. Am. Chem. Soc.* **2015**, *137*, 3779.

(18) Attard, G. S.; Göltner, C. G.; Corker, J. M.; Henke, S.; Templer, R. H. *Angew. Chem., Int. Ed. Engl.* **1997**, *36*, 1315.

(19) Li, C.; Dag, Ö.; Dao, T. D.; Nagao, T.; Sakamoto, Y.; Kimura, T.; Terasaki, O.; Yamauchi, Y. *Nat. Commun.* **2015**, *6*, 6608.

(20) (a) Elliott, J. M.; Attard, G. S.; Bartlett, P. N.; Coleman, N. R. B.; Merckel, D. A. S.; Owen, J. R. *Chem. Mater.* **1999**, *11*, 3602. (b) Yamauchi, Y.; Tonegawa, A.; Komatsu, M.; Wang, H.; Wang, L.; Nemoto, Y.; Suzuki, N.; Kuroda, K. *J. Am. Chem. Soc.* **2012**, *134*, 5100. (c) Takai, A.; Yamauchi, Y.; Kuroda, K. *J. Am. Chem. Soc.* **2010**, *132*, 208.

DOI: 10.1021/jacs.5b06278
J. Am. Chem. Soc. 2015, 137, 11558−11561